Thermopower enhancement in lead telluride nanostructures

Joseph P. Heremans, Christopher M. Thrush, and Donald T. Morelli
Delphi Research Labs, Shelby Township, Michigan 48315
(Received 16 April 2004; revised manuscript received 20 July 2004; published 30 September 2004)

We demonstrate an enhancement in the thermopower of PbTe nanostructures with grain sizes on the order of 30–50 nm, relative to bulk. The enhancement is similar in magnitude to that reported in the literature for $PbTe/PbSe_xTe_{1-x}$ quantum dot superlattices. We provide proof, based on measurements of the transverse Nernst effect, that the enhancement has its origin in electron energy filtering induced by an alteration of the scattering mechanism.

DOI: 10.1103/PhysRevB.70.115334 PACS number(s): 73.63.−b, 72.20.Pa

INTRODUCTION

Over the past decade, a combination of environmental, economic, and technological drivers has led to a resurgence in both the study of thermoelectricity and the search for new materials with superior thermoelectric properties. Both the conversion efficiency ε of thermoelectric power generators, and the coefficient of performance COP of thermoelectric coolers are determined by the thermoelectric figure of merit $Z=S^2\sigma/\kappa$, where S is the Seebeck coefficient or thermopower, σ the electrical conductivity, and κ the thermal conductivity. Current thermoelectric technology (e.g., Bi_2Te_3-based compounds for thermoelectric coolers and PbTe- or SiGe-based compounds for power generation) utilizes materials with $Z.T$ of order unity at their operating temperature T. Roughly a doubling of that number is necessary in order for thermoelectric technology to reach its potential.[1]

Recent work has suggested several routes by which Z may be increased. One of these, the so-called "phonon-glass/electron crystal" concept,[2] envisions materials possessing high electron mobilities and conductivities but with thermal transport properties similar to a glass or amorphous solid. This model seeks to maximize Z by increasing the ratio of the electrical conductivity to the thermal conductivity. Validation of this approach was typified by the observation of a high figure merit above room temperature in filled skutterudites.[3,4] Another approach, originally proposed by Hicks and Dresselhaus,[5] predicts an enhancement in the Seebeck coefficient in systems in which the physical dimensions are smaller than the spatial extent of the electron wave function. In this case the enhancement of S occurs due to an increase in the density of states of electrons near the Fermi level in the solid. Enhanced values of thermopower at ambient temperature have been observed in $PbTe/PbSe_xTe_{1-x}$ quantum dot superlattice structures,[6] which have reached values of $ZT\approx 2$, and in bismuth nanowire composites,[7] the effect in both cases attributed at least partially to quantum confinement. An enhancement in Z has also recently been reported in Bi_2Te_3-based superlattices,[8] but this effect was attributed to a decrease in phonon thermal conductivity at the interfaces.

Here we describe the results of our study of the thermoelectric properties of bulk PbTe-based structures, fabricated using a conventional pressing/sintering process, comprised of nanometer-sized grains. We observe, for grain size in a certain range, an enhancement in the thermopower relative to that of bulk PbTe, and provide evidence that this enhancement is due to yet another mechanism: Selective scattering of electrons depending on their energy. This idea has recently been proposed for metallic structures[9] and was the basis for solid-state thermionic refrigeration.[10] We note that the presence of nanoscale inclusions was reported in a recent paper[11] on PbTe-based high-ZT alloys, although their role is not yet elucidated.

THEORY

In a semiconductor, the thermoelectric power S, the carrier concentration p, and the electrical conductivity σ are functions of the Fermi energy E_F in the system, the carrier effective mass and the carrier scattering relaxation time τ_e, the inverse of the scattering frequency. This frequency in turn contains two factors, the density of initial and final states $g(E)$, and the square of the matrix element of the scattering transition $W(E)$, which is usually assumed to depend on the carrier energy E as $W(E)\propto E^{-\lambda}$ via a *scattering parameter* λ. For scattering of carriers by acoustic phonons $\lambda=0$, whereas for scattering by ionized impurities $\lambda=2$. If we assume that the bands have a parabolic energy-momentum $E(k)$ dispersion relation, $g(E)\propto E^{1/2}$, and this leads to the familiar expression $\tau_e=\tau_o E^{\lambda-1/2}$, where τ_o is an energy-independent scaling coefficient. The assumption that the bands are parabolic does not hold for the valence band of PbTe. In this paper, we use the complete first order nonparabolic expressions for the electrical conductivity, and the Seebeck, Hall, and isothermal Nernst coefficients.[12] In particular, for the valence band in PbTe, the Fermi surfaces are ellipsoids of revolution, and the energy dispersion relation is

$$\frac{\hbar^2 k_l^2}{2m_l^*}+\frac{\hbar^2 k_t^2}{m_t^*}=\gamma(E)=E\left(1+\frac{E}{E_g}\right), \tag{1}$$

where E_g is the direct energy gap of PbTe,[13] and k and m^* are the electron wavevector and effective mass (at $k=0$) along the longitudinal (suffix l) and transverse (suffix t) directions of the ellipsoids. The density of states is[12]

$$g(E) = \frac{\sqrt{2}(m_d^*)^{3/2}}{\pi^2\hbar^3}\gamma'\sqrt{\gamma(E)}, \tag{2}$$

where γ' is the derivative of γ with respect to E, $\hbar$ is the Planck constant, and $m_d^* = \beta^{2/3}(m_l.m_t^2)^{1/3}$ is the density of states effective mass in which we include the degeneracy number β when the Fermi surface contains more than one pocket. It follows from the description of the scattering parameter given above that the energy dependence of τ_e is given by:[12]

$$\tau_e = \tau_o \frac{\gamma(E)^{\lambda-1/2}}{\gamma\prime(E)}. \tag{3}$$

The carrier density is now

$$p = \frac{(2m_d^* k_B T)^{3/2}}{3\pi^2\hbar^3}\int_0^\infty \gamma(z)^{3/2}\left(-\frac{\partial f_0}{\partial z}\right)dz, \tag{4}$$

where k_B is the Boltzmann constant and $z = E/(k_B T)$ is the reduced energy, so that $\gamma(z)$ is given by (1) but with z substituting for E. f_0 is the Fermi-Dirac distribution function. The electrical conductivity is:[12]

$$\sigma = \frac{(2m_d^* k_B T)^{3/2}}{3\pi^2\hbar^3}\frac{e^2}{m_\alpha^*}\int_0^\infty \frac{\gamma(z)^{3/2}}{\gamma'(z)}\tau(z)\left(-\frac{\partial f_0}{\partial z}\right)dz, \tag{5}$$

where e is the carrier charge, m_α^* is the effective mass along the crystallographic direction of the sample studied, or the appropriate average mass for polycrystals, and $\gamma'(z)$ is the derivative of $\gamma(z)$ with respect to z. The low-field ($\mu B \ll 1$) Hall coefficient is

$$R_H = \frac{3K(K+2)}{(32K+1)^2}\frac{1}{pe}\frac{\left(\int_0^\infty \frac{\gamma(z)^{3/2}}{(\gamma'(z))^2}\tau^2(z)\left(-\frac{\partial f_0}{\partial z}\right)dz\right)\left(\int_0^\infty \gamma(z)^{3/2}\left(-\frac{\partial f_0}{\partial z}\right)dz\right)}{\left\{\int_0^\infty \frac{\gamma(z)^{3/2}}{\gamma'(z)}\tau(z)\left(-\frac{\partial f_0}{\partial z}\right)dz\right\}^2}, \tag{6}$$

where K is the effective mass anisotropy coefficient, $K = m_l/m_t$. The Seebeck coefficient is

$$S = \frac{k_B}{e}\left\{\frac{\int_0^\infty \frac{\gamma(z)^{3/2}}{\gamma'(z)}z\tau(z)\left(-\frac{\partial f_0}{\partial z}\right)dz}{\int_0^\infty \frac{\gamma(z)^{3/2}}{\gamma'(z)}\tau(z)\left(-\frac{\partial f_0}{\partial z}\right)dz} - \frac{E_F}{k_B T}\right\}, \tag{7}$$

and the low-field ($\mu B \ll 1$) isothermal Nernst coefficient is

$$N = R_H\sigma\frac{k_B}{e}\left\{\frac{\int_0^\infty \frac{\gamma(z)^{3/2}}{(\gamma'(z))^2}z\tau^2(z)\left(-\frac{\partial f_0}{\partial z}\right)dz}{\int_0^\infty \frac{\gamma(z)^{3/2}}{(\gamma'(z))^2}\tau^2(z)\left(-\frac{\partial f_0}{\partial z}\right)dz} - \frac{\int_0^\infty \frac{\gamma(z)^{3/2}}{\gamma'(z)}z\tau(z)\left(-\frac{\partial f_0}{\partial z}\right)dz}{\int_0^\infty \frac{\gamma(z)^{3/2}}{\gamma'(z)}\tau(z)\left(-\frac{\partial f_0}{\partial z}\right)dz}\right\}. \tag{8}$$

Typically one chooses a value of λ and adjusts the value of the density of states effective mass $m_d^* = (m_l.m_t^2)^{1/3}$ to fit the experimental data to the implicit $S(p)$ curve generated by the nonparabolic formulas. In the case of PbTe, if one fixes $\lambda = 0$ the resulting fitted values of m_d^* are roughly 50% larger than the literature value of density of states effective mass.[13] Alternatively one may use the accepted values[13] for m_d^* and adjust λ to fit the $S(p)$ data on conventional bulk PbTe samples. This procedure yields a good fit to the experimental thermoelectric power data on bulk p-type PbTe for $\lambda \approx 0.7$, and this is the base line shown in Fig. 1.

On three of the samples studied here, rather than simply fitting the $S(p)$ curve by assuming a value of m_d^* and adjusting the value of λ to obtain a good fit, we determine the values of the effective mass and scattering parameter directly by making use of the method of four coefficients. In this method one measures four transport properties on a single sample at each temperature: Conductivity σ (or resistivity ρ), low-field Hall coefficient R_H, thermoelectric power S, and low-field Nernst coefficient N. The experimental values of these four quantities can be substituted into the complete equations (5)–(8)[12] to allow a determination of four independent parameters: (1) carrier mobility μ, which includes the values of τ_0 and m_α^*, (2) carrier concentration p or Fermi energy E_F, (3) density-of-states effective mass m_d^*, and (4) scattering parameter λ. It is our object in the present investigation to demonstrate that by manipulation of the parameter λ via structural engineering at the nanoscale, it is possible to create samples within this semiconductor system with a thermopower that lies above the base-line curve.

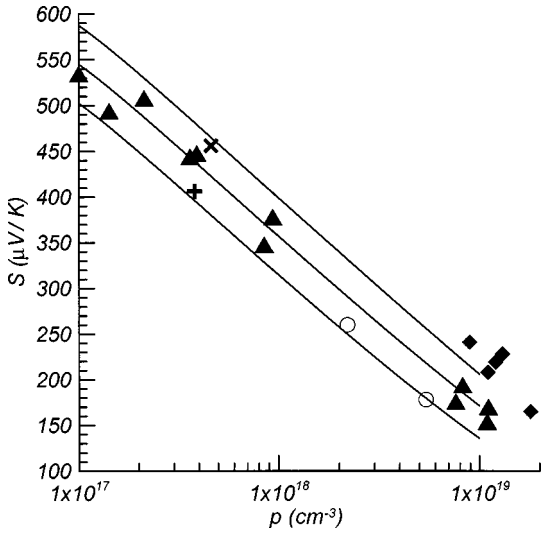

FIG. 1. Thermopower versus hole concentration for p-type PbTe. The bottom solid line represents a fit to literature data on bulk samples using (Ref. 12) a hole effective mass (Ref. 13) $m_d^* \approx 0.16$ and a scattering parameter $\lambda \approx 0.7$. The middle and upper solid lines correspond to the results of the model calculated by incrementing λ by amounts of 0.5 ($\lambda = 1.2$ and 1.7, respectively). The open circles represent data on our bulk samples. (▲) are thermopower data for nanogranular PbTe samples, which exhibit an enhancement similar to that observed in quantum dot PbSeTe superlattices (Ref. 6) indicated by (◆). Thermopower data on coarse-grained (+) and nanogranular (x) PbTe samples containing inclusions of EuTe are also shown. The nanogranular EuTe-containing sample exhibits an enhanced thermopower; the coarse grained sample does not.

EXPERIMENTAL

The samples in this study were made using a standard press and sinter type process. We have fabricated two types of samples: Pure PbTe samples with nanometer-sized grains, and a PbTe sample containing inclusions of EuTe. Starting material was Alfa Aesar pure PbTe, to which was added an appropriate amount of Tl and Te in order to adjust the hole concentration. The starting ingot was pulverized using a mortar and pestle and the coarse-grained powder was placed in a ball mill with n-heptane and zirconia balls. Ball milling proceeded for several days to produce a fine-grained powder, which was then isostatically pressed. The resulting pellets were placed in a quartz tube, subjected to a H_2 thermal cleaning process to remove oxides, and then the ampoule was partially backfilled with a hydrogen atmosphere and sealed. The sample was then sintered for the desired time and at the desired temperature; see Table I for details. We characterized the structure of our nanogranular samples using a Scherrer analysis of the x-ray diffraction line width,[14] using a single crystal InP standard to determine the instrumental line width. Control samples of bulk PbTe with crystallite size in the range of several microns were also fabricated and their thermopower measured to compare with the nanogranular samples. To make the sample containing EuTe inclusions, a process similar to that above was followed, except that 14 mol % $Pb_{0.92}Eu_{0.08}Te$ (prefabricated by melting the constituents at 1000 C and quenching in water) was added in pulverized form to the pulverized PbTe ingot before ball milling. In this case, both a coarse-grained (ball milling for one hour) and a fine-grained (ball milling for 22 hours) sample containing EuTe inclusions were fabricated.

Thermoelectric measurements were taken in a standard liquid N_2 cryostat using a conventional steady state technique. Absolute copper-constantan thermocouples were fixed at two points along the sample length to measure the temperature difference in the direction of heat flow; the copper legs of these thermocouples were also used to measure the Seebeck voltage. Current wires were added to perform conductivity measurements. For transverse Nernst and Hall coefficient measurements a second set of gold wires were placed in a direction transverse to the both the heat flow and the applied magnetic field, which was varied from -1.5 to $+1.5$ T. We report the Hall and the isothermal[15] Nernst coefficient in the low-field limit.

The thermoelectric power of several of our nanostructured samples is shown in Fig. 1 along with the results of Harman *et al.* on PbTe quantum dot superlattice (QDSL) structures.[6] For comparison we also show our results for two bulk PbTe samples that agree very well with the literature values repre-

TABLE I. Parameters of bulk and nanogranular PbTe samples used in Figs. 2 and 3. Samples 98 and 98B were processed together; samples 99B and 100 were processed in two separate batches, designed to be identical.

Sample	Milling time (hours)	Sintering temperature (C)	Sintering time (hours)	Thermopower at 300 K (μV K^{-1})	Hole concentration n (cm^{-3})	X-ray grain size (nm)
66A (+)	1	345	228	406	3.8×10^{17}	$\geqslant$60
66B (×)	22	345	162	456	4.6×10^{17}	44±5
69 (◇)	70	347	161	508	2.1×10^{17}	42±4
98 (■)	70	350	162			
98B (■)	70	350	162	494	1.42×10^{17}	
99B (▲)	72	345	160	189	8.2×10^{18}	36±1.2
100 (▲)	72	345	168	174	7.6×10^{18}	
Bulk PbTe (O)	⋯	⋯	⋯	265	2.2×10^{18}	

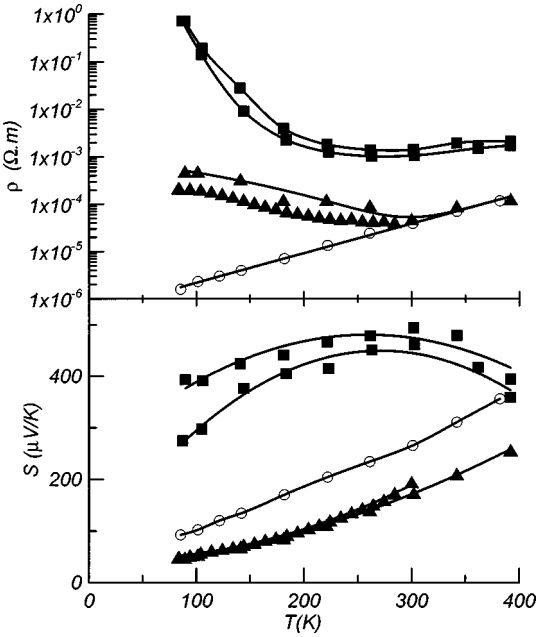

FIG. 2. Electrical resistivity (top panel) and thermopower (bottom panel) versus temperature for two nanogranular PbTe samples with hole concentrations of 2×10^{17} cm^{-3} (■) and 8×10^{18} cm^{-3} (▲; 2 samples). Data on bulk PbTe (○) with a hole concentration of 2×10^{18} cm^{-3} are shown for comparison.

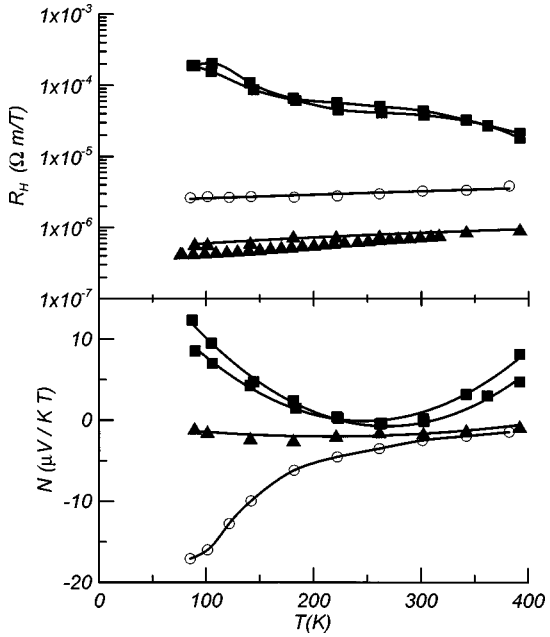

FIG. 3. Hall coefficient (top panel) and isothermal Nernst coefficient (bottom panel) for the same set of samples as in Fig. 2. For bulk PbTe the Nernst coefficient is negative over the entire temperature range. Relative to this bulk sample, for nanogranular samples the Nernst coefficient increases and eventually becomes positive.

sented by the lowest solid line for PbTe. Many, though not all,[16] of our nanostructured samples display an enhancement in S over that of bulk PbTe alloys, with the magnitude of the enhancement quite similar to that exhibited by the QDSL structures. The coarse-grained sample containing EuTe inclusions shows no enhancement, whereas in the fine-grained version of this sample the thermopower is increased by 10%–15%. We thus conclude that the thermopower enhancement that occurs in this sample is due to the nanometer-scale grain structure of the PbTe matrix and not the presence of EuTe inclusions.

Our measurements of the four quantities ρ, S, R_H, and N are shown in Figs. 2 and 3 for four of our nanostructured samples as well as for a sample of bulk PbTe, which shows good agreement with the data of Chernik *et al.*[17] For our nanostructured samples we observe an increase, and in fact for the sample with $n\approx1\times10^{17}$ cm^{-3}, a change in sign to positive values, in the Nernst coefficient. The sign of the Nernst coefficient is independent of the carrier type but is highly dependent on the scattering parameter.

DISCUSSION

The experimental data for the four transport coefficients are fitted as described in the theory section to yield, at each temperature, values of the four material parameters (p,μ,m^*_d,λ). The values of p and μ are very close to what one would obtain from R_H and ρ alone; m^*_d is practically unchanged from its literature value.[13] The carrier scattering parameter λ values determined from these data are shown in Fig. 4 as a function of temperature. The scattering parameter of the nanostructured samples exhibits an increase relative to their bulk counterparts for comparable hole concentrations. This is displayed very clearly in Fig. 5 where $\lambda(p)$ is plotted at 300 K for both bulk and nanostructured samples. Whereas bulk PbTe exhibits a scattering parameter in the range of 0.2–0.7, we find that this parameter increases to the range of 0.7–1.1 in the nanostructured samples.

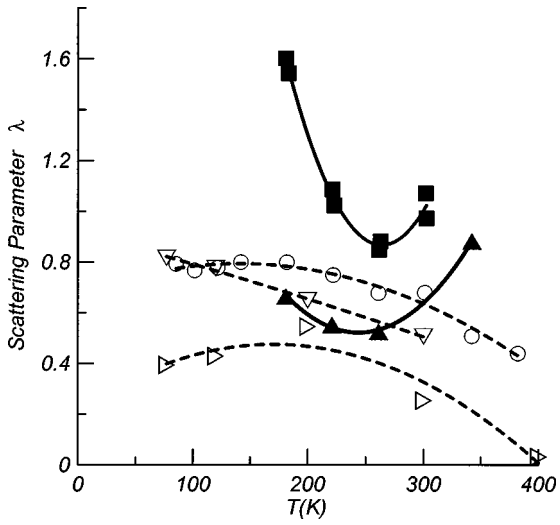

FIG. 4. Electron scattering parameter λ as a function of temperature, for two nanogranular PbTe samples with hole concentrations of 2×10^{17} cm^{-3} (■) and 8×10^{18} cm^{-3} (▲). Data on bulk PbTe samples (dashed lines) with a hole concentration of 1×10^{18} cm^{-3} (▽), 2×10^{18} cm^{-3} (○), and 7×10^{18} cm^{-3} (▷) are shown for comparison.

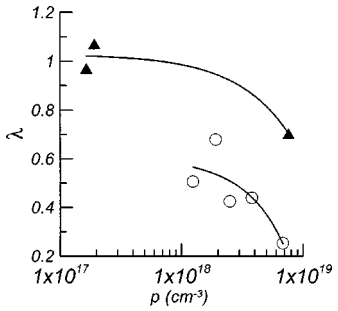

FIG. 5. Electron scattering parameter λ at 300 K as a function of hole concentration in bulk (○) and nanogranular (▲) PbTe. For nanogranular samples λ is enhanced relative to bulk PbTe of the same hole concentration.

We ascribe the enhancement of S to an enhanced λ. Since the samples studied here contain nanometer-sized features one can speculate whether the enhancement in S is due to a modification of the DOS of electrons in these systems due to quantum confinement, as has been suggested for the QDSL structures. We point out, however, that quantum confinement is expected to evolve for structures with features less than 10 nanometers, whereas the feature size in our structures is much larger, on the order of 30–50 nanometers (see Table I), on the order of the electron mean free path. This is consistent with the fact that a change is observed in λ and not in m^*_d. Another possibility arises from the probable presence of strain in the material due to the ball-milling process. The expected effects of strain are: A broadening of the x-ray diffraction (XRD) spectra, a change in the actual carrier density, and a change in λ. The presence of residual strain does therefore not affect our argument, which holds whatever the mechanism responsible for the increase in λ in nanometer size structures. An increase in the magnitude of λ results in a stronger energy dependence of electron scattering; in effect a "filtering" process by which higher energy electrons are more efficiently separated from lower energy electrons, leading[9] to an increase in thermopower.

CONCLUSION

While the condition for quantum confinement and an altered DOS is a physical dimension smaller than the spatial extent of the electron wave function, the condition for scattering-induced enhancement of the thermopower is a physical dimension less than the electron mean free path. This is considerably less restrictive from the practical point of view as it implies conventional manufacturing methods such as that used in this study may be employed to positively influence the thermoelectric properties of PbTe alloys. We speculate that the increase in electron scattering parameter with decreasing grain size is due to the influence of grain boundary scattering, and possibly to strain. While this scattering also decreases the electron mobility and electrical conductivity, it is suggested this may be in part offset by a decrease in thermal conductivity.

ACKNOWLEDGMENT

The authors acknowledge support from the Delphi Corporation for this work.

[1] J. P. Heremans, in *Thermoelectric Materials 2003-Research and Applications: MRS Symposium Proceedings, Boston, December 2003*, edited by G. S. Nolas, J. Yang, T. P. Hogan, and D. C. Johnson (Materials Research Society Press, Pittsburgh, PA, 2004), pp. 3–14.

[2] G. A. Slack, in *CRC Handbook of Thermoelectrics*, edited by D. M. Rowe (CRC Press, Boca Raton, FL, 1995), p. 407.

[3] J.-P. Fleurial, A. Borshchevsky, T. Caillat, D. T. Morelli, and G. P. Meisner, *Proceedings of the 16th International Conference on Thermoelectrics* (IEEE Press, Pennington, NJ, 1996), p. 91.

[4] B. C. Sales, D. Mandrus, and R. K. Williams, Science **272**, 1325 (1996).

[5] L. D. Hicks and M. S. Dresselhaus, Phys. Rev. B **47**, 12727 (1993).

[6] T. C. Harman, P. J. Taylor, M. P. Walsh, and B. E. LaForge, Science **297**, 2229 (2002).

[7] J. P. Heremans, C. M. Thrush, D. T. Morelli, and M-C. Wu, Phys. Rev. Lett. **88**, 216801 (2002).

[8] R. Venkatasubramanian, E. Siivola, T. Colpitts, and B. O'Quinn, Nature (London) **413**, 597 (2001).

[9] D. Vashaee and A. Shakouri, Phys. Rev. Lett. **92**, 106103 (2004).

[10] G. D. Mahan and L. M. Woods, Phys. Rev. Lett. **80**, 4016 (1998).

[11] K. F. Hsu, S. Loo, F. Guo, W. Chen, J. S. Dyck, C. Uher, T. Hogan, E. K. Polychroniadis, and M. G. Kanatzidis, Science **303**, 818 (2004).

[12] Yu. I. Ravich, B. A. Efimova, and I. A. Smirnov, *Semiconducting Lead Chalcogenides* (Plenum, New York, 1970).

[13] H. Preier, Appl. Phys. **20**, 189 (1979).

[14] B. D. Cullity, *Elements of X-Ray Diffraction* (Addison-Wesley, Reading, MA, 1956).

[15] We measure the adiabatic Nernst coefficient and apply the correction factor given in I. M. Tsidil'kovskii, *Thermomagnetic Effects in Semiconductors* (Academic, New York, 1962), p. 181.

[16] We show the results on all the samples measured, illustrating the degree of repeatability of the results, but were not able to correlate the observed enhancement to a particular parameter in the sample preparation.

[17] A. Chernik, V. I. Kaidanov, M. I. Vinogradova, and N. V. Kolomoets, Sov. Phys. Semicond. **2**, 645 (1968).